MISSION AND ECONOMIC ANALYSIS OF AIRCRAFT WITH NATURAL LAMINAR FLOW

Kai Wicke , Martin Kruse , Florian Linke
DLR - German Aerospace Center
kai.wicke@dlr.de; martin.kruse@dlr.de; florian.linke@dlr.de

Keywords: *natural laminar flow, mission analysis, fleet analysis, life-cycle cost, air transportation system*

Abstract

The objective of this paper is the analysis and assessment of a natural laminar flow (NLF) aircraft with forward swept wings on air transport system level. In particular, the impact on fuel efficiency on single missions and on airline operational level as well as economic metrics like the net present value are of special interest. The net economic benefit for an aircraft operator gained by the operation of a NLF aircraft concept is shown, considering real-world route network conditions including existing flight routes with their respective frequencies. The focus will be on short-to-medium haul operations, i.e., aircraft similar to current state of the art 150 passenger seated aircraft. During the analysis process tools for aircraft design, mission simulation and computation as well as life-cycle cost assessment will be used.

1 Introduction

The minimization of aircraft operating cost is a major objective of today's airlines. Especially the fuel burn related cost rises due to higher fuel prices and the inclusion of the air transport sector in the European emission trading scheme. Beside the economical aspects, airlines and aircraft manufacturers are pushed towards more environmental friendly aircraft. Considering the high demand for air travel and the associated growing percentage of aircraft operations on anthropogenic carbon dioxide emissions, the demand for a more environmental responsible behavior of airlines will arise. The defined economical and environmental goals in the Vision 2020 of the Advisory Council for Aeronautical Research in Europe (ACARE) represent a first approach to solve these problems. However, the ambitious goals cannot be achieved by today's aircraft design philosophies and more radical changes and improvements are necessary.
The application of natural laminar flow (NLF) on transport aircraft is a promising future technology offering significant potential for increasing aircraft fuel efficiency [1, 2]. Simultaneously, the climate impact of aircraft can be reduced since less emissions are produced. Beyond that, NLF is a prospective technology that could be integrated in a next generation short-to-medium range aircraft. As outlined in a number of studies, a fuel burn improvement in the order of 10-15% [3, 4, 5] is possible by generating laminar flow on an aircraft wing. However, the existing numbers are only valid for optimum boundary conditions like operation at design range. In common airline operation, in-service degradation will emerge from off-design conditions, for example the operation on short ranges or the influence of operational risks to laminar flow (like weather effects or contamination) on aircraft performance. This in turn affects aircraft economy and reduces laminar flow benefits. Various papers deal

with the impact of operational risks on laminar flow and how this affects possible fuel burn improvements [6, 7]. But the aspect of rising maintenance effort and the implication on the aircraft's economic viability is usually neglected.

This paper presents an enhanced system analysis process to determine the potential fuel burn improvement and the economic net benefit of an aircraft designed for NLF on air transport system (ATS) level. To account for variable operational boundary conditions, different assessment scenarios are considered and analyzed for their impact on aircraft profitability.

1.1 Approach for Analysis

The applied approach for analyzing NLF aircraft on ATS level is displayed schematically in Fig. 1. The shown process also reflects the organization of the paper. The starting point for the assessment is the aircraft design and aerodynamic optimization performed by DLR Institute of Aerodynamics and Flow Technology [8]. To account for NLF in early design stages, a simplified laminar-turbulent transition model is introduced into the preliminary aircraft design process. Aerodynamic and performance data resulting from the aircraft design are used in subsequent analysis tools to determine key performance indicators on various system levels.

The first two performance indicators are related to fuel efficiency on single mission level and fuel efficiency under realistic air transport network conditions. Finally, the economic efficiency is derived based on the results from previous analysis steps.

2 NLF Aircraft Design

Conventional jet-powered transport aircraft feature backward swept wings in order to reduce wave drag and thus enable efficient transonic cruise flight. For typical leading edge sweep angles of 25° to 30° and Reynolds numbers of $20 \cdot 10^6$ and above, laminar-turbulent transition takes place close to the leading edge due to strong amplification of cross flow or attachment line instabilities [2, 9]. DLR's concept for a transonic NLF transport aircraft introduces a forward swept, tapered wing planform [10]. Hereby, the leading edge sweep angle is reduced to obtain conditions under which NLF becomes realizable [11]. Furthermore, the forward swept wing's shock sweep angle is large enough to maintain cruise Mach numbers comparable to those of today's reference configurations. The combination of the forward swept wing (FSW) with NLF offers a gain in flight performance. Since NLF is a passive flow control technology, no further systems need to be installed. The main disadvantage of FSWs is their tendency for aeroelastic divergence, causing additional weight for structural reinforcements [12]. Approaching this problem, carbon fibre reinforced plastic (CFRP) can be used for aeroelastic tailoring to affect the deformational behavior of the wing systematically [13, 14]. At the same time, the material properties of CFRP can be used to lessen the weight penalty and to obtain a high surface quality with respect to roughness and waviness [15, 16]. Today's aluminum manufacturing techniques with its rivets and surface discontinuities seem not sufficient for realizing adequate surface qualities for NLF.

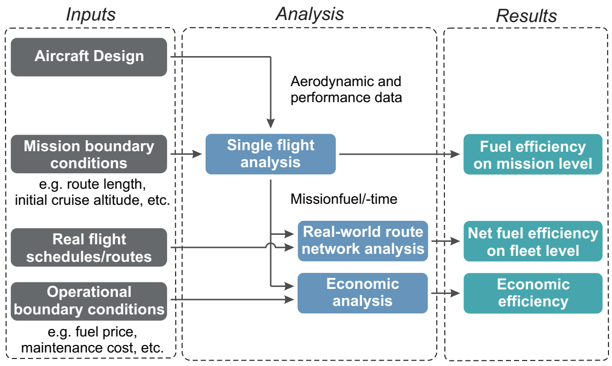

Fig. 1. Analysis approach.

The FSW-NLF aircraft as well as the reference aircraft are designed at the DLR Institute of Aerodynamics and Flow Technology with the preliminary aircraft design software PrADO (Preliminary Aircraft Design and Optimization Program [17, 18]). Detailed information about the preliminary aircraft design

Tab. 1. Concept of operation.

Requirement	Value
Design range	4,815 km
Payload	14,250 kg (150 Pax incl. baggage)
Cruise Mach number	0.78
Take-off field length	7,000 ft
Landing field length	5,500 ft

Tab. 2. Configuration characteristics.

Parameter	Reference	FSW-NLF
Lift-to-drag ratio	16.4	19.2
Wing area	122.6 m^2	132.0 m^2
Span	34 m	35.8 m
OEW	41.35 t	43.71 t
MTOW	72.55 t	73.36 t

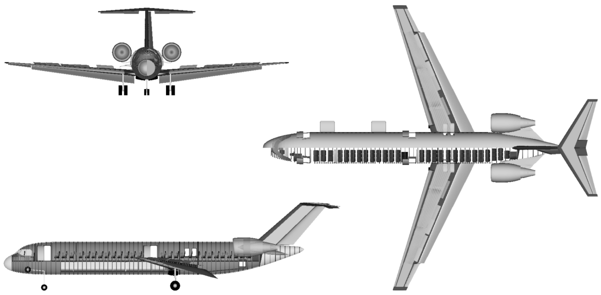

Fig. 2. FSW-NLF aircraft design with PrADO.

used in this study and additional configuration studies are published in [8]. In order to guarantee the comparability of both aircraft, the FSW-NLF aircraft concept of operation corresponds to the reference aircraft (see Tab. 1). The reference configuration represents an aircraft design similar to current state of the art short-to-medium range aircraft with turbulent wing design.

Beside forward swept wings, the NLF aircraft features a T-tail and rear-mounted engines, as shown in Fig. 2. This design is chosen in order to create a clean wing with optimum laminar flow conditions. NLF is maintained over the forward part of the wing by an appropriate wing section design, leading to a maximum transition location of about 55 % local wing depth in the outer wing area. Due to this aerodynamic design, the lift-to-drag ratio is increased by 17.1 % compared to the reference aircraft. The T-tail configuration would also allow the installation of new engine concepts with very high bypass ratios, like geared turbofans or propfans. However, the T-Tail and the FSW design results in a 5.7 % higher operating empty weight (OEW). Even the CFRP wing can only partially compensate the weight penalty. Compared to the reference aircraft, the maximum take-off weight (MTOW) increases only by 1.1 %, justified by a lower required mission fuel of the FSW-NLF aircraft.

With respect to the leading edge high lift system, the aircraft is equipped with smart leading edge devices [19, 20] instead of conventional slats, providing a stepless and gapless wing surface. At the current state of preliminary aircraft design, a protection system against wing contamination is not regarded. In order to guarantee an optimum performance either a wing protection system should be installed in the aircraft or the wing leading edge needs to be cleaned before the flight. One solution to preventing contamination would be the installation of Krueger-Slats. During the critical phases of take-off and landing, the slat would shield the leading edge against pollutants. Triggered by design, standard Krueger high lift devices imply steps and gaps that cause pre-mature transition. Thus, this solution is discarded since the analyzed aircraft deploys NLF on the upper and lower wing surface. An overview of further promising protection techniques can be found in [21].

2.1 Modeling of Laminar Flow in PrADO

In order to consider NLF in early aircraft design stages, it is necessary to implement a simplified laminar-turbulent transition model in the design process. In PrADO, aerodynamic calculations are based on a multi-lifting line method. To account for NLF wings, the computation of the zero lift drag has been modified. The implemented model uses a flat-plate analogy for friction drag and considers laminar-turbulent transition with a weighted equivalent skin-friction coefficient published in [22].

$$C_{fe}(\eta) = \underbrace{FF_{la}\frac{1.328}{Re^{1/2}(\eta)}\frac{x_T}{c}(\eta)+}_{laminar} \underbrace{FF_{tu}\frac{0.074}{Re^{1/5}(\eta)}\left(1-\frac{x_T}{c}(\eta)\right)}_{turbulent} \quad (1)$$

The equivalent skin friction coefficient considers the pressure drag from viscous effects with the form factors FF_{la} for laminar boundary layers as well as FF_{tu} for turbulent boundary layers. The zero lift drag of the wing is then estimated with a prescribed laminar-turbulent transition, dependent on the local Reynolds number and the integration of Eq. 1 in spanwise direction. This approach indirectly includes the aircraft's flight velocity and cruise altitude since it is based on Reynolds number. It is assumed that up to a Reynolds number of $25 \cdot 10^6$, a $55\,\%$ extension of laminar flow exists. Between Reynolds numbers of $25 \cdot 10^6$ and $35 \cdot 10^6$, a linear reduction of transition location is used in the model. These prescribed values are based on the results of the natural laminar airfoil design for selected design Mach numbers, selected leading edge sweep, local lift coefficients and local airfoil thickness. This approach includes indirectly the complex influences of the local lift coefficient $c_l(\eta)$ and the local airfoil thickness $t/c(\eta)$ to laminar-turbulent transition. Furthermore, no differentiation of the upper and lower wing with respect to laminar-turbulent transition is considered. This means the equivalent skin-friction coefficient $C_{fe}(\eta)$ has to be perceived as an average value of the upper and lower wing.

The form factors for laminar and turbulent boundary layers are derived from high-fidelity airfoil analysis with a variation of forced laminar-turbulent transition. These investigations were done for a conventional turbulent airfoil and a designed NLF airfoil. The selected Mach number was below the critical Mach number of these airfoils to avoid any wave drag influence. With the selected values for the form factors of FF_{la}=1.15 for laminar boundary layers and FF_{tu}=1.35 for turbulent boundary layers, a good agreement with the airfoil analysis was achieved.

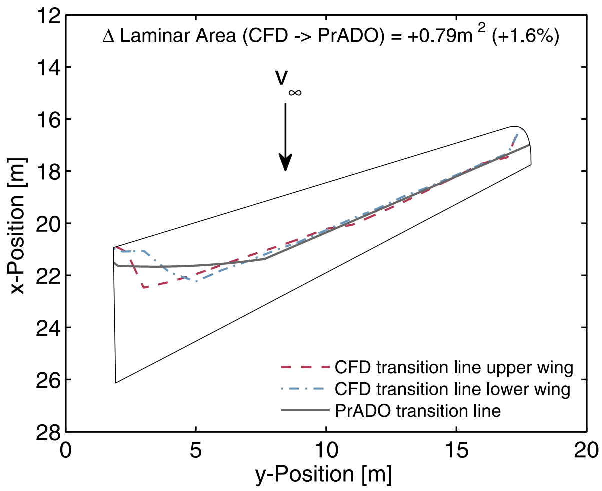

Fig. 3. Comparison of spanwise transition position, PrADO transition model vs. high-fidelity results.

The transition line that results from the application of the simplified transition model in PrADO is shown in Fig. 3. A comparison with transition line prediction from high-fidelity coupled aero-structural simulations performed in [8] show a fair agreement. Although the PrADO transition model does not differentiate between the upper and lower side of the wing, the occurring differences to the high-fidelity simulations in terms of laminar area is only $1.6\,\%$. It should be noted that the high level of agreement is achieved by calibration of the laminar-turbulent transition model using data from wing section design. Therefore, the model's validity is limited to cruise flight conditions of the current FSW-NLF design. More detailed information about the aerodynamic design and optimization can be found in [8]. Since the assumptions for the extension of laminar flow used in preliminary aircraft design have been confirmed by high-fidelity results, the aerodynamic performance maps from PrADO are used in the subsequent ATS analysis.

3 Mission Simulation and Analysis

3.1 Single Mission Analysis

The provided aerodynamic and performance data from the aircraft design are used as an input for further analysis. In order to consider the payload-range characteristics and the flight performance of the reference and the FSW-NLF aircraft within the single mission and real-world route network analysis, flight mission simulations are performed. The goal is to determine required mission fuel and time for different stage lengths, initial cruise altitudes (ICA) and flow conditions on the NLF wing. This is done by applying parts of the CATS [1] simulation chain [23, 24], which was developed at DLR for assessing the climate impact of aircraft for different mission profiles and aircraft designs. The simulation tool computes three-dimensional trajectories with distribution of mission fuel and mission time for all routes of interest based on a total energy model. The aerodynamic and engine performance maps resulting from the aircraft design are used to account for the performance of both aircraft during the mission simulation.

Routes between 250 and $4,750\,\mathrm{km}$ (step size $250\,\mathrm{km}$) are simulated for the reference aircraft and the FSW-NLF configuration for determining the required mission fuel. The computed trajectories are analyzed for the relative change in mission fuel due to the use of NLF. Depending on the mission length and the respective loading condition of the aircraft, an appropriate ICA is selected. Both aircraft start their initial cruise at the same altitude. Thus, the atmospheric flight conditions and the transport performance are identical. Typical cruise flight levels on very short missions ($< 750\,\mathrm{km}$) are based on original flight data from the Eurocontrol Central Flow Management Unit (CFMU) [2]. On longer routes, ICA is selected in such a manner that the lift coefficient is close to the design value.

To account for in-service degradations of the FSW-NLF aircraft, three different aerodynamic quality scenarios are modeled. Beside a first operational scenario that assumes the highest available aerodynamic performance with optimum laminar flow (approximately 11.6% of the aircraft's surface flow is laminar), the second scenario accounts for reduced aerodynamic performance (approximately 5.8% of the aircraft's surface flow is laminar). This case reflects a NLF-wing that is operated only with 50% of its available laminar area. Influencing factors for laminar efficiency are e. g. icing conditions, cloud encounters, rain or insects [7, 21, 25, 26]. Finally, the third scenario represents a worst case operation with a fully turbulent wing on all flight segments.

The laminar-turbulent transition model used in the preliminary aircraft design is only valid within a limited lift coefficient and Mach range due to its calibration with high-fidelity methods. Extension of NLF is essentially dependent on the pressure distribution and the local Reynolds number. To consider this fact in the mission simulation, three boundary conditions must be fulfilled to assure laminar flow. 1) Cruise altitudes must be higher than $31,000\,\mathrm{ft}$. Below this altitude, a combination of too high Reynolds numbers as well as weather effects cause improper conditions for laminar flow. 2) The Mach number should be between 0.76 and 0.8. Off-design Mach numbers will evoke a pressure distribution not adequate to achieve maximum laminar flow. 3) The lift coefficient c_L should be in a range from 0.45 to 0.55. A deviation from this range might lead to a reduced laminar flow area with degraded flight performance. An assessment of the aerodynamic performance showed that within the defined ranges, no significant changes in laminar flow expansion exist [8].

During trajectory calculation, the mission simulator analyzes the actual flight conditions and monitors the boundary conditions for compliance. In case of violating one of the boundary conditions, the mission simulator

[1] DLR project CATS - Climate compatible Air Transport System

[2] Eurocontrol CFMU data internally provided by the DLR project "Weather & Flying"

automatically changes from the provided laminar aerodynamic performance map to the turbulent one. It should be noted that in real flight operations, the change from laminar to full turbulent flow under off-design conditions would be a continuous process and not as sudden as modeled in this study.

An example of a trajectory calculated for a $2,750\,\mathrm{km}$ mission with the conditions of altitude, Mach number and lift coefficient is shown in Fig. 4. The flight phases where laminar flow conditions are fulfilled are shaded in orange.

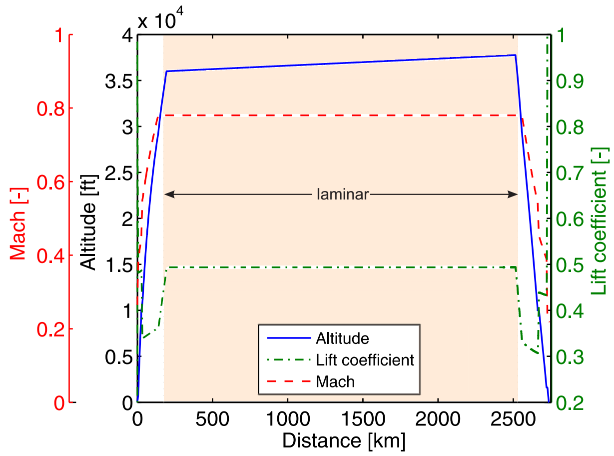

Fig. 4. Trajectory for a $2,750\,\mathrm{km}$ mission with conditions of altitude, Mach number and lift coefficient.

The final results of single mission computations are shown in Fig. 5 as mission fuel change relative to the reference aircraft for all analyzed routes. It is apparent that the change in mission fuel strongly depends on the flown stage length. On missions shorter than $500\,\mathrm{km}$, no benefit exists. The main reason for this effect is an ICA below $31,000\,\mathrm{ft}$. Consequently, the turbulent performance map is used in the mission simulation. The maximum fuel saving potential is reached on long routes. With up to $8.5\,\%$ mission fuel reduction, the results are in the order of magnitude of other studies [2, 3, 27]. This value shrinks to $2\,\%$ for missions around $750\,\mathrm{km}$. Taking in-service degradation of the FSW-NLF aircraft into account, the potential fuel saving is substantially reduced to $0.3\,\%$ on short missions and $4.5\,\%$ for a distance of $4,750\,\mathrm{km}$.

An operation with fully turbulent wing shows no benefit for routes shorter than $2,500\,\mathrm{km}$. Starting here, the fuel burn is in the order of the reference aircraft with a small advantage on long missions. This can be ascribed to lower induced drag caused by the higher wing span of the FSW-NLF aircraft.

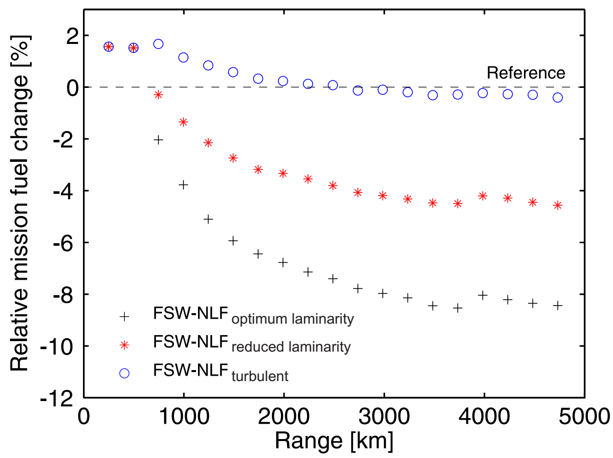

Fig. 5. Relative change of mission fuel on single mission basis for operating laminar aircraft instead of typical short-to-medium range aircraft.

3.2 Real-World Route Network Analysis

Beside the relative fuel burn savings on single missions, an aircraft operator is also interested in how a new aircraft influences fuel consumption on operational level. For this reason, it is necessary to evaluate the NLF aircraft under realistic air transportation network conditions by considering the typical flight routes with their respective frequencies. For this purpose, all scheduled flights served by Airbus A320 for a time period of one week are gathered from Airport Data Intelligence (ADI). The distribution of flown missions with their respective flight frequencies is plotted in Fig. 6.

The data show an average mission length of $1,300\,\mathrm{km}$, with $99\,\%$ of flights being operated on routes below $4,000\,\mathrm{km}$. It becomes apparent that under realistic air network conditions, the typical operation of today's short-to-medium haul aircraft totally differs from their design point. For an aircraft with NLF technology, this

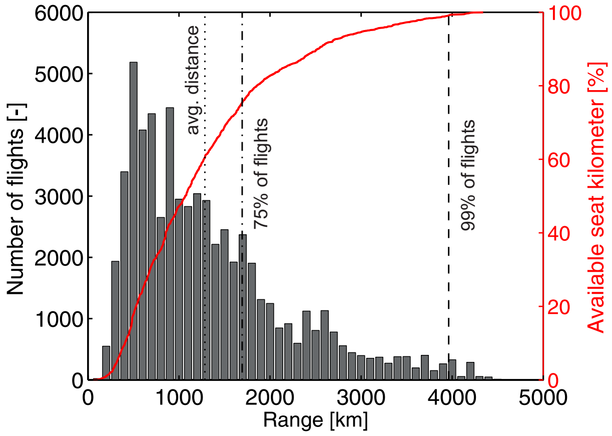

Fig. 6. Mission length for typical short-to-medium range aircraft with their respective flight frequencies.

fact implies an additional in-service degradation since NLF can deploy its full potential only during cruise. Short missions with their relatively small portion of cruise flight cut down the fuel burn improvement. In normal airline operation this effect is even intensified by the high number of flights on these segments.

To analyze the total fuel change under real-world operational conditions, the reference aircraft was gradually substituted by the NLF configuration (solid black line in Fig. 7). The level of introduction is indicated as share of flights, starting with NLF-operation on long ranges. The change in required fuel on operational level (ΔOF) is calculated as described in Eqn. 2, where i represents the number of flights on each route flown, m the number of routes and SMF the respective single mission fuel of the route. The number of routes with their frequencies are taken from ADI. Data for SMF are based on results from the single mission analysis.

$$\Delta OF = \frac{\left(\sum\limits_{seg=1}^{m} i_{seg} \cdot SMF_{seg}\right)_{NLF}}{\left(\sum\limits_{seg=1}^{m} i_{seg} \cdot SMF_{seg}\right)_{Ref.}} - 1 \quad (2)$$

The achievable reduction of fuel on operational level depends on the share of flights operated by the FSW-NLF aircraft (see Fig. 7). For example, if $30\,\%$ of the flights are substituted with the NLF aircraft, this will result in a fuel consumption that is reduced by $4\,\%$. Looking at the cumulated fuel change curve for optimum laminar flow, an improvement of required fuel can be noticed, up to the maximum achievable saving of $5.7\,\%$ at a NLF flight share of $76.1\,\%$. This would result in operating the NLF aircraft from $600\,\mathrm{km}$ up to the longest flown distance. An operation below that point (stage length $< 600\,\mathrm{km}$) causes a marginal benefit reduction down to $5.5\,\%$. Substituting $50\,\%$ of all flights by NLF aircraft already results in $5.2\,\%$ fuel burn improvement. That is $90.8\,\%$ of the maximum saveable fuel. Taking a reduced aerodynamic efficiency into account, the achievable saving on airline level is decreased down to $2.6\,\%$.

The presented fuel benefits may slightly vary from airline to airline, since the airline business model has an impact on distribution of mission length and flight frequencies.

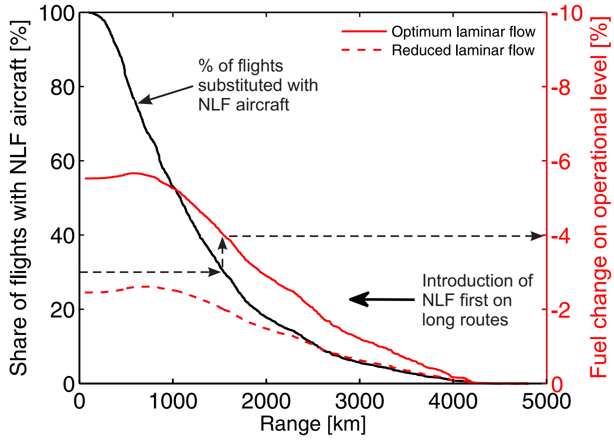

Fig. 7. Fuel change on airline operational level due to gradually substitution of the reference aircraft by NLF aircraft.

4 Economic Analysis

The economic viability of a new aircraft concept is essential from an operator's point of view. The direct operating cost (DOC) represent a very common metric for comparing the economic value of aircraft [28, 29]. In general, the area of validity of this method is the period with steady state cost, i. e. , between 5 to 10 operating years.

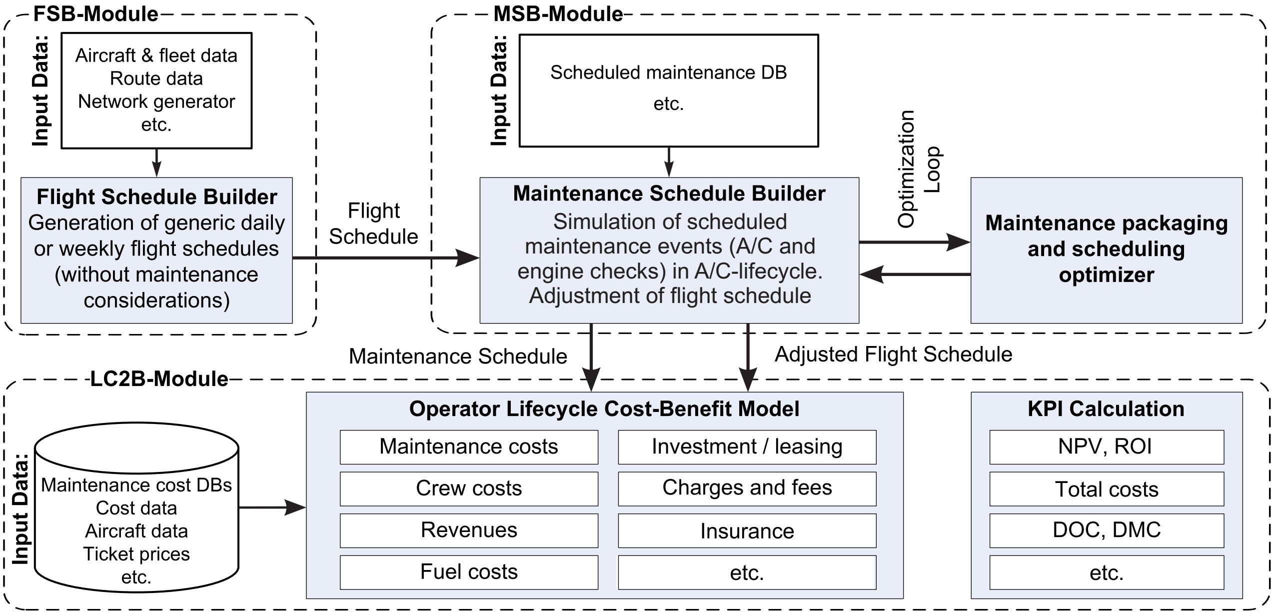

Fig. 8. AirTOBS program structure [30, 31].

The chosen year should represent a year with average cost. DOC are computed for a certain mission with a defined yearly utilization on a flight-cycle or flight-hour basis.

In this study, the economic analysis is extended to a life-cycle cost benefit analysis in order to model the impact of NLF on the economic performance more accurately. The applied method models all relevant cost elements from an operator's point of view as well as the airline revenues along the system life-cycle. The actual time of occurrence of the cost and revenue elements is captured to account for the time value of money. This allows for a more flexible evaluation of new technologies, since single cost elements (e. g. maintenance activities) are adjustable by time and cost. All values are escalated over the aircraft life-cycle to account for inflation.

The life-cycle cost calculations are performed with AirTOBS (Aircraft Technology and Operations Benchmark System) developed at DLR Institute of Air Transportation Systems [30, 31]. A schematic overview of the program structure can be found in Fig. 8. The tool itself comprises a flight schedule builder (FSB), a maintenance schedule builder (MSB) and the life-cycle cost benefit module (LC2B). The FSB generates aircraft life-cycle flight schedules based on inputs like aircraft dependent mission flight time, taxi times or turnaround time. Within the next step, the flight schedule is adjusted by maintenance events. This is done by the MSB which simulates maintenance events on discrete, rule-based events (aircraft and engine checks). Each event is triggered by flight cycles, elapsed flight hours or a combination of both. Event characteristics like check interval, downtime, man-hours or cost are based on Aircraft Commerce data [32] and stored in a data bank. With the available data, the MSB creates a maintenance plan with all occurring maintenance events in the aircraft life-cycle.

The economic assessment takes place in the LC2B-module. For the assessment and the comparison of different aircraft, the Net Present Value (NPV) is chosen as key performance metric. The NPV covers all costs and revenues with respect to an investment. All cash flows C_t in the respective operating year t of the aircraft life-cycle are discounted to the reference year at a discount rate r (see Eq. 3). The discount rate represents the minimum acceptable return on capital. A NPV of zero reflects a case where the strived return on capital is reached. The factor C_0

in Eq. 3 represents the initial investment.

$$NPV = C_0 + \sum_{t=1}^{T} \frac{C_t}{(1+r)^t} \tag{3}$$

The focus of this study is the added value for the aircraft operator due to the introduction of new aircraft. Based on the calculation for the reference aircraft, the impact of NLF is shown as ΔNPV whereby a positive result reflects an economic benefit for the operator of the NLF aircraft.

In order to account for uncertainties in the life-cycle cost analysis, different scenarios are applied to cover a wide band of operational boundary conditions (see Tab. 3). The NPV assessment is performed for the design range as well as a route mix. Evaluating only the design range would not be accepted by an aircraft operator, since the typical utilization of the aircraft differs significantly from the design point. The route mix composition for the LCC assessment with its respective mission length and relative flight frequencies is derived from Fig. 6. Fuel data that correspond to the ranges used for the economic analysis are gathered from the single mission simulation. Likewise, the aerodynamic performance scenarios for optimum and reduced laminarity are included in the NPV calculations.

Aircraft maintenance events are modeled as discrete, rule-based events. In this study, especially the change of maintenance effort and cost linked to the NLF operation are of interest. As mentioned in Section 3.1, the contamination of the wing with pollutants may strongly affect aircraft performance. From an airline perspective, it does not seem to be a solution to remove pollutants before each flight. Especially on short-to-medium range operation, a longer turnaround time might result in decreased utilization. Therefore, the shortest possible maintenance interval would be a nightly cleaning during the ramp check. To estimate the required amount of cleaning material, time and cost, the area affected by contamination was derived. Based on price lists for certified aircraft cleaning materials, different cost scenarios for a single cleaning process were derived (see Tab. 3). Cleaning time was estimated from time specifications found for aircraft cleaning [33].

Tab. 3. Assessment scenarios.

Parameter	**NLF aircraft scenarios**
Mission length	Design Range / Route Mix
Aerodynamic performance	Optimum and reduced
Ramp check cost (RCC)	unchanged
	+5 %/ + 20 %/ + 50 %/ + 100 %
Aircraft price	unchanged / +5 %/10 %
Fuel price	65 US$/140 US$/210 US$

To estimate the initial investment of the airline due to the aircraft acquisition, it is assumed that the aircraft price correlates with technology improvements. Using formulas given in [34], the aircraft price can be estimated by the advancement in aircraft system performance. In this case, reductions in future costs (e. g. lower DOC per revenue seat kilometer and better fuel efficiency) are purchased by the airline through higher investment cost. Other factors that will influence pricing are the manufacturer's non recurring and recurring cost to develop and produce NLF aircraft. Taking the mentioned aspects into account, three theoretic prices for the NLF aircraft were derived based on manufacturer price lists for today's short-to-medium range aircraft.

The historic development of airline fuel cost represents one key factor for the application of laminar flow technology. With the world's growing energy consumption and limited resources, the fuel price could become an even more important factor for airline economics. To cover this important economic aspect, three different fuel price models reaching from 65 US$/barrel to 210 US$/barrel are used in the assessment to cover possible future trends. These scenarios are adopted from the Energy Information Agency (EIA).

Combining the different assessment scenario parameters, the composition of high fuel price, optimum aerodynamic performance, operation at design range, same aircraft price and no change in maintenance effort may be seen as best operational environment for the FSW-NLF aircraft. Thus, the worst case evaluation scenario would be a low fuel price with reduced aerodynamic performance, operation on a route mix, a 10 % higher aircraft price and higher maintenance expenditure.

In Fig. 9 - 12, the relative change in NPV for a life-cycle of 20 years is shown for the different assessment scenarios. All figures show the positive effect of laminar flow on fuel cost in terms of an increasing ΔNPV with higher fuel prices. Fig. 9 highlights that the ΔNPV is maximized for operation at design range with optimum laminar flow and no changes in cost related to FSW-NLF aircraft operation. Economic viability is still given for the lowest fuel price scenario combined with 5 % higher investment cost and a doubling of ramp check cost (RCC). A further escalation of aircraft price causes a change in sign of ΔNPV for the low fuel price. In this case, the fuel price threshold for becoming an profitable system lies between 80 US$/barrel and 113 US$/barrel, depending on RCC escalation.

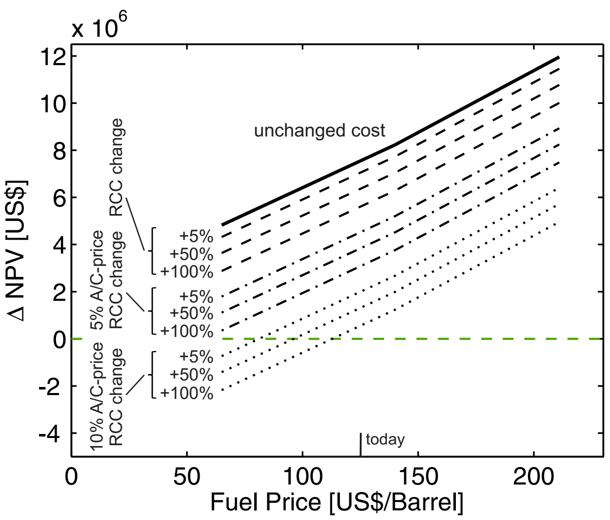

Fig. 9. ΔNPV for NLF operation at design range with optimum laminar flow for different cost scenarios.

The impact of reduced aerodynamic performance on ΔNPV can be seen in Fig. 10. The cutback of ΔNPV is in the order of 47 %. At the same time, the allowable investment and maintenance cost for the FSW-NLF aircraft is shifted to lower values. A flattening of the curves also becomes apparent. Comparing the scenario for 5 % higher RCC combined with a 10 % higher aircraft price in Fig. 9 and Fig. 10, it becomes obvious that the incremental fuel price shifts from 80 US$/barrel to 180 US$/barrel in case of reduced aerodynamic performance operation.

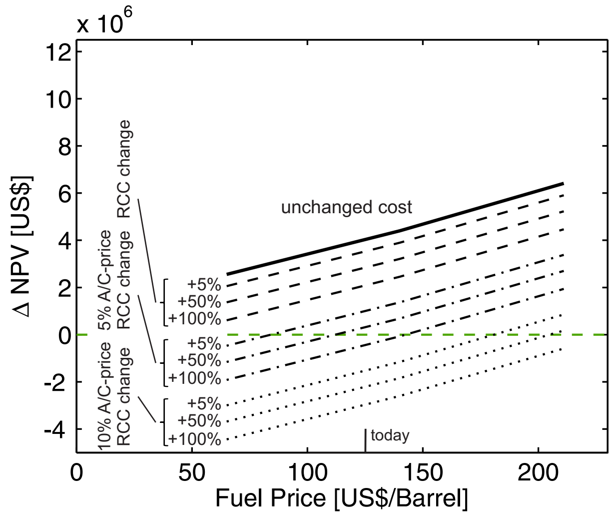

Fig. 10. ΔNPV for NLF operation at design range with reduced laminar flow for different cost scenarios.

According to Fig. 11, the operation of the FSW-NLF aircraft on a realistic airline route mix provokes a further reduction of economic advantage. For optimum laminar flow conditions, positive values of ΔNPV only exist for scenarios where the RCC is varied and no additional change in capital cost incur. From that point on, a positive ΔNPV can only be achieved when the fuel price shifts to higher marginal values. Furthermore, all RCC scenarios with a 10 % increase of aircraft price result in negative ΔNPV. Similar to the operation at design range, a reduction of laminar flow causes a negative impact on economic effectiveness (see Fig. 12). Based on today's fuel price, the utilization of the FSW-NLF aircraft would only be profitable for an airline when the additional RCC remains under 50 % and the manufacturer keep the quoted aircraft price unchanged. For all other scenario combinations plottet in this figure, the FSW-NLF concept would not be an alternative for an airline from a business point of view.

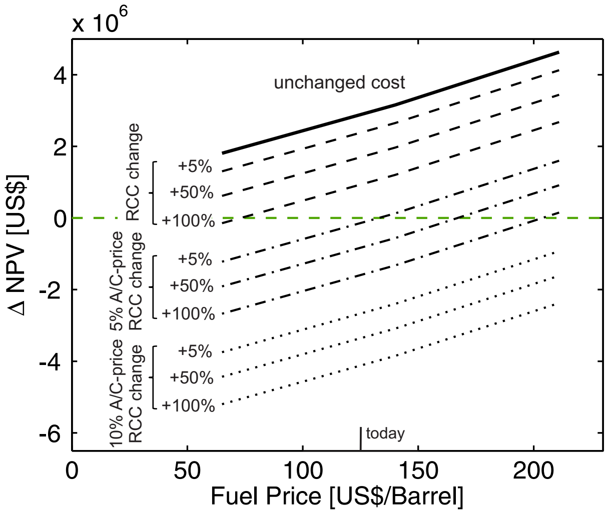

Fig. 11. ΔNPV for NLF operation on a route mix with optimum laminar flow for different cost scenarios.

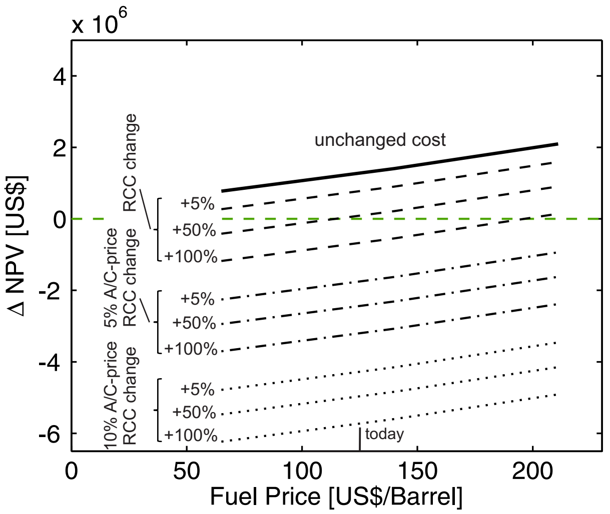

Fig. 12. ΔNPV for NLF operation on a route mix with reduced laminar flow for different cost scenarios.

A NPV-isolines plot as shown in Fig. 13 allows to determine all combinations of aircraft price and RCC where the NPV is equal to zero. In this example, the ΔNPV turns positive for all combinations below an aircraft price increase of $7.9\,\%$ with no further RCC and a $4.9\,\%$ higher aircraft price with a $100\,\%$ escalation of RCC. Beyond that, all pairs of values for percentage deviation from that line can be derived.

To analyze how the fuel price influences the trade-off of allowable expenditure that will result in a positive ΔNPV, isolines for the different fuel price scenarios for an operation at design range with reduced aerodynamic performance are applied to Fig. 14. All cost escalation combinations beneath the limiting curve of ΔNPV=0 result in positive ΔNPV in favor of the FSW-NLF aircraft. The figure again shows that a rising fuel price allows for an increase of additional cost to achieve economic viability.

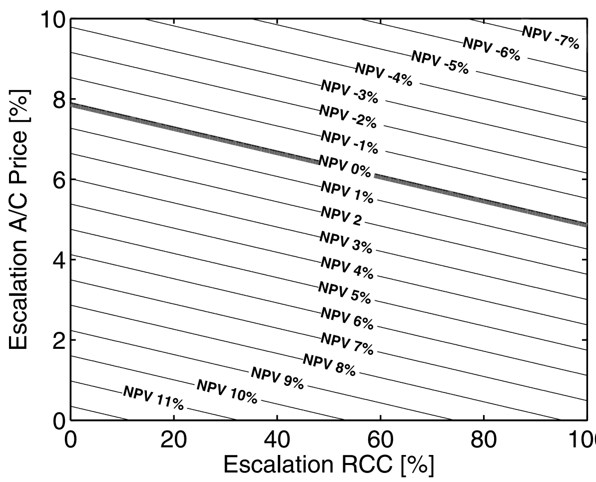

Fig. 13. NPV-isolines for aircraft price variation and RCC cost variation (design range with reduced laminar flow - fuel price scenario 140 US$/barrel).

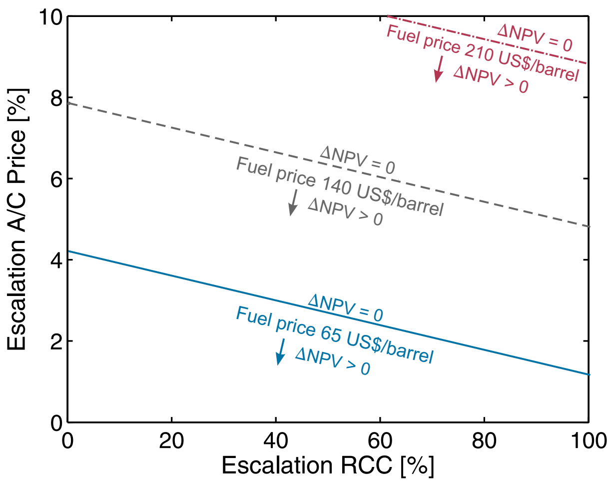

Fig. 14. Aircraft price and RCC cost combinations resulting in ΔNPV=0 with variation of fuel price at design range and reduced laminar flow.

Comparing Fig. 14 and Fig. 15, the isolines for ΔNPV=0 are shifted significantly to lower cost for an operation on a realistic route mix. This is due to the reduced fuel saving potential already mentioned in Section 3.2. As a consequence, the beneficial effect of fuel saving on economic performance is compensated earlier by the negative effects of increased aircraft price and RCC.

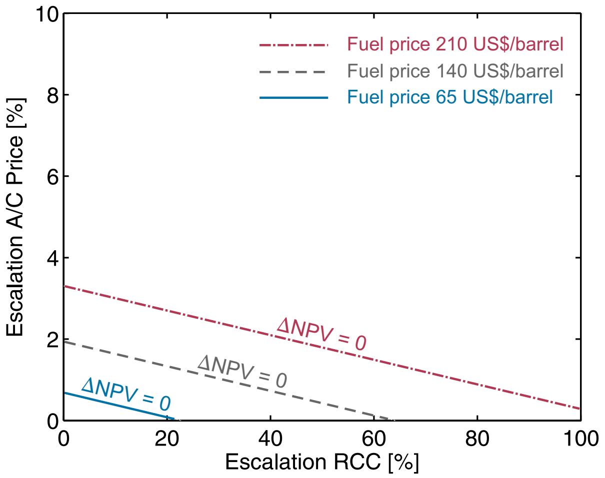

Fig. 15. Aircraft price and RCC cost combinations resulting in ΔNPV=0 with variation of fuel price for route mix operation and reduced laminar flow.

5 Conclusion and Outlook

This paper describes an enhanced system analysis process to analyze and assess the effects on fuel efficiency and airline economics due to the introduction of FSW-NLF aircraft on air transport system level. The applied process chain comprises tools for single mission fuel analysis, real world route network analysis and economics calculations. The assessment of fuel efficiency on single mission basis showed an advantage of up to $8.5\,\%$ by operating the FSW-NLF aircraft instead of the reference configuration. It was found that the possible fuel benefit strongly depends on mission length as well as on in-service degradations used to simulate aerodynamic deterioration of the FSW-NLF aircraft. In order to assess the achievable fuel benefit on airline operational level, real-world routes with their respective flight frequencies were considered in the analysis. These investigations demonstrated a fuel burn improvement of up to $5.7\,\%$ due to the utilization of the FSW-NLF aircraft. Beside the analysis of fuel efficiency, the economic viability of NLF aircraft for different operational scenarios was of interest. According to Fig. 9-12, the beneficial effect for an airline's economy also strongly depends on operational boundary conditions such as aerodynamic quality, fuel price and non-fuel related cost like aircraft price or maintenance cost.

In future studies, the focus will be directed more towards operational aspects and risks to laminar flow. Particularly, effects that could evoke premature transition or a complete loss of laminar flow (e. g. insects, cloud encounter, ice crystals) and their impact on fuel planning need to be investigated and considered in more detail in the analysis process. This will require an estimation of the operational risks impact on fuel burn during each phase of flight. In a next step, these influences need to be included in the aircraft economy assessment. Furthermore, it is planned to extend the maintenance analysis. So far, the maintenance effort with respect to CFRP-structures or long time behavior of high quality surfaces necessary for laminar flow is not considered.

References

[1] ICAO, *ICAO Environmental Report 2010 - Aviation and climate change*, Montreal, Quebec, Canada, 2010.

[2] Rossow CC. Aerodynamics - A discipline swept away? *Aeronautical Journal*, Vol. 114, No. 1160, pp. 599-609, 2010.

[3] Allison E, Kroo I, Suziki Y and Martins-Ricas H. Aircraft conceptual design with natural laminar flow. *27th International Congress of the Aeronautical Sciences (ICAS)*, Nice, France, 2010.

[4] Holmes B J and Obara C J. Flight research on natural laminar flow applications. *Natural laminar flow and laminar flow control*,

ICASE/NASA LaRC Series, Editors: Barnwell, R.W. and Hussaini, M.Y., Springer-Verlag, New York, pp. 72-142, 1992.

[5] Schrauf G. Status and perspectives of laminar flow. *Aeronautical Journal*, Vol. 109, No. 1102, pp. 639-644, 2005.

[6] Young T M and Fielding J P. Flight operational assessment of hybrid laminar flow control (HLFC) aircraft. *Aerodynamic drag reduction technologies: proceedings of the CEAS, DragNet European Drag Reduction Conference*. Potsdam, Germany, Editor: P. Thiede, Springer-Verlag, Berlin-Heidelberg-New York, pp. 99-106, 2001.

[7] Elsenaar A and Haasnoot H N. A survey on Schiphol airport of contamination of wing leading edges of three different aircraft types under operating conditions. *Proceedings of the 1st European Forum on Laminar Flow Technology*. Hamburg, Germany, DGLR-Bericht 92-06, Deutsche Gesellschaft für Luft- und Raumfahrt, Bonn, pp. 256-261, 1992.

[8] Kruse M, Wunderlich T and Heinrich L. A conceptual study of a transonic NLF transport aircraft with forward swept wings. *30th AIAA Applied Aerodynamics Conference*, New Orleans, Louisiana, AIAA 2012-3208, 2012.

[9] Green J E. Laminar flow control - Back to future?. *AIAA 38th Fluid Dynamics Conference and Exhibit*, Seattle, Washington, AIAA-2008-3738, 2008.

[10] Seitz A, Kruse M, Wunderlich T, Bold J and Heinrich L. The DLR project LamAiR: Design of a NLF forward swept wing for short and medium range transport application. *29th AIAA Applied Aerodynamics Conference*, Honolulu, Hawaii, AIAA 2011-3526, 2011.

[11] Redeker G and Wichmann G. Forward sweep - A favorable concept for a laminar flow wing. *Journal of Aircraft*, Vol. 28, No. 2, pp. 97-103, 1991.

[12] Horstmann K H and Streit T. Aerodynamic wing design for transport aircraft - today. *Hermann Schlichting - 100 Years*. Springer-Verlag, Berlin, Heidelberg, pp. 130-144, 2009.

[13] Weisshaar T A. Aeroelastic tailoring of forward swept composite wings. *Journal of Aircraft*, Vol. 18, No. 8, pp. 669-676, 1981.

[14] Librescu L and Khdeir A A. Aeroelastic divergence of swept-forward composite wings including warping restraint effect. *AIAA Journal*, Vol. 26, No. 11, pp. 1373-1377, 1988.

[15] Joslin R D. Overview of laminar flow control. *NASA/TP-1998-208705*, Langley Research Center, Hampton, Virginia, 1998.

[16] Holmes B J and Obara C J. Observation and implications of natural laminar flow on practical airplane surfaces. *Journal of Aircraft*, Vol. 20, No. 12, pp. 993-1006, 1983.

[17] Werner-Westphal C, Heinze W and Horst P. Multidisciplinary integrated preliminary design applied to future green aircraft configurations. *45th AIAA Aerospace Sciences Meeting and Exhibit*, Reno, Nevada, AIAA 2007-655, 2007.

[18] Werner-Westphal C, Heinze W and Horst P. Multidisciplinary integrated preliminary design applied to unconventional aircraft configuration. *Journal of Aircraft*, Vol. 45, No. 2, pp. 581-590, 2008.

[19] Monner H P, Kintscher M, Lorkowski T and Storm S. Design of a smart droop nose as leading edge high lift system for transportation aircraft. *50th AIAA/ASME/ASCE/AHS/ASC Structures, Structural Dynamics, and Materials Conference*, Palm Springs, California, AIAA 2009-2128, 2009.

[20] Kintscher M, Monner H P and Heintze O. Experimental testing of a smart leading edge high lift device for commercial transportation aircraft. *27th International Congress of the Aeronautical Sciences (ICAS)*, Nice, France, 2010.

[21] Humphreys B. Contamination avoidance for laminar flow surfaces. *Proceedings of the 1st European Forum on Laminar Flow Technology*. Hamburg, Germany, DGLR-Bericht 92-06, Deutsche Gesellschaft für Luft- und Raumfahrt, Bonn, pp. 262-273, 1992.

[22] Raymer, D P. *Aircraft design: A conceptual approach*. Third edition, American Institute of Aeronautics and Astronautics, 1999.

[23] Koch A et al. Integrated analysis and design environment for a climate compatible air transport system. *9th AIAA Aviation Technology, Integration, and Operations Conference*, Hilton Head, South Carolina, AIAA 2009-7050, 2009.

[24] Koch A et al. Climate impact assessment of varying cruise flight altitudes applying the CATS

simulation approach. *CEAS 3rd Air and Space Conference*, Venice, Italy, 2011.

[25] Nastrom G D, Holdeman J D and Davis R E. Cloud-encounter and particle-concentration variabilities from GASP data. *NASA/TP-1981-1886*, Langley Research Center, Hampton, Virginia, 1981.

[26] Holmes B J et al. Flight investigation of natural laminar flow on the Bellanca Skyrocket II. *SAE Paper 830717*, 1983.

[27] Wilson R A L and Jones R I. Project design studies on aircraft employing natural and assisted laminar flow technologies. *SAE Paper 952038*, 1995.

[28] Liebeck R. Advanced subsonic airplane design & economic studies. *NASA*, Lewis Research Center, 1995.

[29] American Airlines. A new method for estimating current and future transport operating economics. *U.S. Department of Commerce*, Tulsa, 1978.

[30] Schilling T, Hölzel N and Langhans S. Cost-benefit evaluation of aircraft maintenance base-check downtime and cost. *3rd International Air Transport and Operations Symposium (ATOS)*, Delft, Netherlands, 2012.

[31] Hölzel N B, Schilling T and Neuheuser T. System analysis of prognostic and health management systems for future transport aircraft. *28th International Congress of the Aeronautical Sciences (ICAS)*, Brisbane, Australia, 2012.

[32] Aircraft Commerce. Aircraft owners & operators guide: A320 family. *Aircraft Commerce*, Issue No. 44, 2006.

[33] Airbus. Getting hand-on experience with aerodynamic deterioration. *Airbus - Flight Operations Support - Customer Services Directorate*, Issue 2, 2001.

[34] Lee J J, Lukachko S P, Waitz I A and Schafer A. Historical and future trends in aircraft performance, cost, and emissions. *Annual review of energy and environment*, Vol. 26, pp. 167-200, 2001.

Copyright Statement